An Alcohol Extract Prepared From the Male Flower of Eucommia Ulmoides Oliv. Promotes Synovial Cell Apoptosis, Inhibits Osteoclast Differentiation and Ameliorates Bone Destruction in Rheumatoid Arthritis

Yan Zhang
Shanghai University of Traditional Chinese Medicine
Jian-Ying Wang
Shanghai University of Traditional Chinese Medicine
Hao Wang
Shanghai University of Traditional Chinese Medicine
Xiao-Yun Chen
Shanghai Longhua Hospital affiliated to Shanghai University of TCM
Lei Zhang
Shanghai University of Traditional Chinese Medicine
Ying Yuan (yyin921@163.com)
Shanghai University of Traditional Chinese Medicine

Research Article

Keywords: Rheumatoid arthritis, Eucommia ulmoides Oliv., CIA rat, bone metabolism, NF-κB signaling pathway

Posted Date: July 20th, 2021

DOI: https://doi.org/10.21203/rs.3.rs-676535/v1

An alcohol extract prepared from the male flower of *Eucommia ulmoides* Oliv. promotes synovial cell apoptosis, inhibits osteoclast differentiation and ameliorates bone destruction in rheumatoid arthritis

Yan Zhang[a#], Jian-Ying Wang[b#], Hao Wang[c], Xiao-Yun Chen[d], Lei Zhang[b], Ying Yuan[a*]

[a] School of Traditional Chinese Materia Medica, Shanghai University of Traditional Chinese Medicine, No.1200 Cailun Road, Pudong District,201203, Shanghai, China.
[b] Shanghai Innovation Center of TCM Health Service, Shanghai University of Traditional Chinese Medicine, No.1200 Cailun Road, Pudong District, 201203, Shanghai, China.
[c] Shanghai Key Laboratory of Formulated Chinese Medicines, Shanghai University of Traditional Chinese Medicine, No.1200 Cailun Road, Pudong District,201203, Shanghai, China.
[d] Shanghai Longhua Hospital affiliated to Shanghai University of TCM, Rheumatoid Department, No.725 South Wanpin Road, Xuhui District,200232, Shanghai, China.
[#]These authors contributed equally to this article.
* Corresponding author
Ying Yuan, School of Traditional Chinese Materia Medica, Shanghai University of Traditional Chinese Medicine, No.1200 Cailun Road, Pudong District,201203, Shanghai, China. Tel.: 13564474631. E-mail address: yyin921@163.com

Abstract

Background: Rheumatoid arthritis (RA) is a chronic systemic autoimmune disease with a complex pathogenesis and is dominated by synovial hyperplasia and bone destruction. Previous research has shown that the male flower of *Eucommia ulmoides* Oliv. (EF) can exert effect on the inflammation caused by rheumatoid arthritis. However, the effect of EF on synovial cell apoptosis and bone destruction on RA have yet to be investigated. In this study, the effects of the synovial cell apoptosis of the male flower of *Eucommia ulmoides* Oliv.(EF) on human fibroblast-like synoviocyte -RA (HFLS-RA) cells, the osteoclast differentiation of EF on RAW264.7 cells and the bone destruction of effects of EF on collagen-induced arthritis (CIA) rats were explored.

Materials and methods: *In vitro*, we investigated the anti-proliferative and pro-apoptotic effects of EF on HFLS-RA cells by immunofluorescence assays, flow cytometry, RT-qPCR (Real-time quantitative polymerase chain reaction), and western blotting. We investigated the differentiation into osteoclasts effects of EF on RAW264.7 cells by the TRAP staining and western blotting. *In vivo*, we used a rat model of collagen-induced arthritis (CIA) to investigate the relative effects of EF on anti-arthritis activity, the toe swelling arthritis score, the serum levels of metabolic bone factors, and pathological conditions. Micro-computed tomography (micro-CT) was used to scan ankle joints while the mRNA and protein levels of factors related to the NF-κB pathway were determined by RT-qPCR and western blotting, respectively. Finally, the main chemical components of EF were identified by HPLC (High Performance Liquid Chromatography).

Results: EF inhibited the proliferation of synovial cells and promoted apoptosis in a dose-dependent manner, inhibited the differentiation of osteoclast by inhibiting activation of the NF-κB pathway. We also found that EF reduced articular inflammation in CIA rats, inhibited the expression of pro-angiogenic factors, and delayed the destruction of articular cartilage and bone. Our data indicate that EF acts *via* a mechanism related to bone metabolism that is induced by the NF-κB pathway.

Conclusions: Our findings indicate that EF exerts a potential therapeutic effect on rheumatoid arthritis. Our research will help to elucidate the potential pharmacological mechanisms associated with the beneficial effects of EF and provide an experimental basis for the application of EF in future clinical treatments.

Keywords: Rheumatoid arthritis; *Eucommia ulmoides* Oliv.; CIA rat; bone metabolism; NF-κB signaling pathway

Introduction

Rheumatoid arthritis (RA) is an autoimmune disease that is dominated by chronic multiarticular inflammation and bone destruction. The main pathological features of RA include the proliferation of synovial cells, pannus formation, the destruction of cartilage and bone, and even joint deformity. These changes cause a great deal of inconvenience to the patients affected by this disease and create a significant burden with regards to daily life and work activities. RA is a very common global disease; the World Health Organization (WHO) lists RA as one of the most troublesome global diseases [1]. Although diagnostic methods and treatments have improved significantly over recent years, studies have found that the currently available drugs for RA are mainly disease-relieving anti-rheumatic drugs (such as methotrexate), non-steroidal anti-inflammatory drugs (NSAIDs), glucocorticoids (such as dexamethasone), and other biological agents [2]. With regards to joint inflammation, even if synovial inflammation has been controlled during the late stages of rheumatoid arthritis, the destruction of bone can still cause irreversible damage to the joints. Therefore, inhibiting the early proliferation of synovial cells, and slowing pannus formation, may represent potential treatment methods with which to reduce the subsequent erosion of cartilage and bone. Traditional Chinese medicine (TCM) has achieved certain curative effects in the treatment of RA. Previous studies have found that three different extracts from *Eucommia ulmoides* Oliv. can significantly inhibit bone destruction, synovial inflammation, and systemic inflammation [1].

The NF-κB pathway plays an important role in a variety of immune diseases. When stimulated by interleukin-1 (IL-1), tumor necrosis factor (TNF-α) and cells activate IκB kinase (Iκκs); this kinase phosphorylates, ubiquitinates and then degrades the IκB protein. This leads to the dissociation of IκB from NF-κB in the cytoplasm. Once transferred into the nucleus, NF-κB regulates the transcription of a range of target genes, promotes angiogenesis and the expression of cytokines such as IL-1β and vascular endothelial growth factor (VEGF) , and thus exacerbates attacks on the bone and cartilage in RA [3]. Therefore, inhibition of the NF-κB pathway may represent a potential therapeutic approach with which to control the bone destruction of RA.

There is increasing evidence that Chinese herbal medicines are valuable resources for the treatment of some intractable diseases[4-5]. *Eucommia ulmoides* Oliv. (EU) is a traditional Chinese medicinal plant. The bark and leaves of EU are used widely in TCM clinics. The active ingredients of EU are able to reduce blood pressure, improve immune function, and can exhibit anti-aging, anti-inflammatory, and anti-tumor effects. EU is one of the most commonly prescribed TCM ingredients used for the clinical treatment of RA [6-7]. In a previous study, we found that an alcohol extract prepared from the bark of *Eucommia ulmoides* Oliv. (EB) was able to inhibit the proliferation of synovial cells in human rheumatoid arthritis (RA-FLS) *in vitro* and promote their apoptosis. *In vivo*, the swelling and arthritic scores of a collagen-induced rheumatoid arthritis (CIA) rat model were reduced when treated with EB; pathological analysis further suggested that synovial inflammatory infiltration was improved and

pannus formation was alleviated [8]. However, EB grows slowly and resources are incredibly scarce; consequently, there is an urgent need to identify alternatives. The male flower of *Eucommia ulmoides* Oliv. (EF) is relatively rich in terms of resources. Previous research has shown that EF can exert anti-inflammatory, analgesic, anti-bacterial, and other pharmacological effects, including immunoregulation [9]. EF is often used for daily health care, and the prospects are good for developing and utilizing EF in a wide range of clinical applications [10]. In previous published articles, we have preliminarily discussed the effects of EB, EL and EF on improving inflammation in CIA rats. EF and EB have similar functions. We found that EF can reduce the expression of TNF-α and NO in synovial cells and improve the articular inflammation in CIA rats *in vivo* [11]. Therefore, on this basis, this study further explored the mechanism of EF on promoting synovial cell apoptosis and inhibiting the bone destruction, explored whether the effect of EF on synovial cell apoptosis and bone destruction on CIA rats is related to the activation of NF-κB pathway and provided experimental basis for the further application of EF. Currently, there are few studies on the treatment of RA by EF, however, the effects of EF on RA have yet to be confirmed.

In this study, we investigated the effect of EF on the proliferation, migration, and apoptosis in human fibroblast-like synoviocyte cells-RA (HFLS-RA); we investigated the effect of EF on the osteoclast differentiation in RAW264.7 cell; these cells are the main causes of tissue injury and distortion in the joints in RA. We also evaluated the effects of EF on inflammatory bone destruction *via* the NF-κB pathway in a rat model of CIA. Our goal was to provide an experimental basis for the rational application of EF in future clinical RA treatments and to provide a modern interpretation of its pharmacological mechanism.

Materials and Methods

Main reagents and antibodies

Dulbecco's modified Eagle medium (DMEM) was purchased from Gibco (Grand Island, NY, USA,11995065). Human TNF-α was purchased from Peprotech (Rocky Hill, NJ, USA,315-01A). Anti-NF-κB-phospho-p65, anti-phospho-Iκκαβ, anti-phospho-IκBα, anti-cleaved Caspase3, anti-Bax, and anti-Bcl-2 receptor antibodies, along with protease inhibitors, were purchased from Cell Signaling Technology (Beverly, MA, USA,3033,2697,2859,9644,5023,15071). Bovine type II collagen (CII) and complete Freund's adjuvant (CFA) were provided by Chondrex Inc. (Chondrex, Seattle, WA, USA,20021,7001). Rat ELISA assay kits were obtained from Kenuodi Biological Technology Co. Ltd. (Kenuodi, China, TF129, TF176, TF143, TF181). EZ-press RNA Purification Kit, 4 × Reverse Transcription Master Mix, and 2 × SYBR Green qPCR Master Mix, were purchased from EZBioscience (EZBioscience, Roseville, USA, B0004DP, A0010CGQ, A0012-R2). Methotrexate (MTX) purchased from Shanghai Shang yao Xinyi Pharmaceutical Factory Co., Ltd. Specifications: 2.5mg/ tablet, 16 tablets/bottle, batch number 036170604.

Ethanol extracts of plant material

EF was purchased from Shanghai Kangqiao Chinese Medicine Tablet Co., Ltd., (Shanghai, China) and was identified as dried male flower of *Eucommiaul moides Oliv.* by Associate Professor Wu Jin-Rong from the Department of Pharmacognosy, School of Chinese Materia Medica, Shanghai University of Chinese Medicine. EF was extracted twice using 70% ethanol (1:8, w/v for 1 h), filtered and vacuum dried to await experimentation. The concentration of the extract was 1 g/mL [11]. Based on the preliminary experiments conducted by our project team in the early stage and the basic research in the early stage, the effect was obvious when the drug concentration was 1 g/mL. Therefore, in vivo experiment, the concentration of the high dose was set at 1 g/mL and the low dose was set at 0.5 g/mL. To qualitatively investigate the main constituents of ethanol extracts from EF, we performed HPLC analysis.

Cell culture and cell viability assays for HFLS-RA cells

HFLS-RA cells were purchased from Huatuo Biotechnology Co., Ltd. (Guangzhou, China). These cells were cultured in DMEM supplemented with 10% FBS and 1% penicillin-streptomycin solution (hereafter referred to as "standard growth medium") in a humidified atmosphere of 5% CO_2/95% air at 37°C (referred to hereafter as "standard culture conditions"). The Cell Counting Kit-8 (CCK-8) assay (Dojindo, Kunamoto, Japan) was used in accordance with the manufacturer's instructions, to determine cell viability. HFLS-RA cells were pre-incubated for 24 h or 48 h with EF at various concentrations (0, 25, 50, 100, 200, 400, 800, and 1600 μg/mL) in 96-well plates. Then, 10% CCK8 medium was added to the 96-well plates and a microplate reader was used to measure the absorbance at 450 nm. The relative rate of cell viability was expressed as a proportion (%) of the control group.

Animals

Thirty Wistar rats, weighing 120±10 g, were purchased from Beijing CRL Laboratory Animal Co., Ltd. (China); the animal certificate number was SCXK (Beijing) 2016-0011. All animal procedures were performed according to the ethical guidelines of the Laboratory Animal Welfare and Animal Experimental Ethics Committee of Shanghai University of Traditional Chinese Medicine (Approval number: PZSHUTCM18122823).

Cell proliferation and the CCK-8 assay

HFLS-RA cells were inoculated in 96-well plates. Cells were pre-incubated for 24 h with EF at various concentrations (0, 25, 50, 100, 200, 400, 800, 1600, 2000 μg/mL) with or without TNF-α (10 ng/mL) for 24h. Following stimulation, 10% CCK8 medium was added to the 96-well plates. A microplate reader was then used to measure the absorbance at 450 nm. The relative rate of cell viability was then expressed as a proportion (%) of the control group.

Cell colony forming assay

Rat tail collagen was diluted to 3% with PBS and added to a 6-well plate. HFLS-RA cells were cultured in serum-free DMEM for 24 h in 6-well plates (in triplicate). After starvation, the cells were either left untreated (as negative controls) or supplemented with various concentrations of EF (0, 100, 200, 400, 800, and 1600 μg/mL). Cells were treated for 2 days and then cultured for 7 days. Following culture, the cells were fixed with 4% pre-cooled paraformaldehyde and stained with 0.5% crystal violet. The crystal violet was eluted with 70% ethanol, and the eluent was transferred to a 96-well culture plate. The optical density (OD) was then read at 595 nm. The relative rate of cell viability was then expressed as a proportion (%) of the control group.

Cell proliferation and the EdU assay

HFLS-RA cells were cultured in serum-free DMEM for 24 h. Following the cells were either left untreated (as negative controls) or supplemented with various concentrations of EF (400, 800, and 1600 μg/mL) and TNF-α (10 ng/mL) for 24 h. Cell proliferation assays were then performed using a BeyoClick™ EdU Cell Proliferation Kit with Alexa Fluor 594 (Beyotime) in accordance with the manufacturer's instructions.

Cell migration and invasion tests

An Ibidi plugin was placed in a 24-well culture plate. HFLS-RA cells were then inoculated into the plugin and either left untreated (as negative controls) or supplemented with various concentrations of EF (400, 800, and 1600 μg/mL) and TNF-α (10 ng/mL) for 24 h. Scratch areas were photographed with an inverted microscope. Cells were also implanted in Transwell chambers and either left untreated (as negative controls) or supplemented with various concentrations of EF (400, 800, and 1600

μg/mL) and TNF-α (10 ng/mL) for 24 h. Following treatment, the cells were fixed with 4% paraformaldehyde and stained with 0.1% crystal violet solution. The cells were then placed onto a glass slide and five fields from each group were selected for photography under an inverted microscope. Cells were eluted with 33% acetic acid in 96-well plates and the OD value was read at 570 nm. The relative rate of cell viability was expressed as a proportion (%) of the control group.

Flow cytometric analysis of apoptosis

HFLS-RA cells were pre-incubated for 24 h with EF at various concentrations (400, 800, 1600 μg/mL) with or without TNF-α (10 ng/mL). As recommended by the manufacturers of the Annexin V-FITC/PI apoptosis detection kit, cells were re-suspended with binding buffer, and mixed with 5 μL of Annexin V-FITC and PI. Cell apoptosis was then detected by flow cytometry analysis.

Detection of the mRNA levels of various inflammatory factors in HLFS-RA cells by RT-qPCR assays

HFLS-RA cells were cultured in 6-well plates and treated with TNF-α (10 ng/mL) and EF (400, 800, and 1600 μg/mL) for 24 h. RNA was extracted with EZ-press RNA Purification Kit and cDNA was synthesized with 4 × Reverse Transcription Master Mix. Real-time quantitative polymerase chain reaction (RT-qPCR) was then used to quantify gene expression levels. RT-qPCR was performed using 2 × SYBR Green qPCR Master Mix on an ABI Prism 7500 qPCR system (Thermo Fisher Scientific) with the following cycling conditions: initial denaturation at 95°C for 5 min, followed by 40 cycles of 95°C for 10 s, 60°C for 30 s, and a final extension at 72°C for 90 s. The primers used for RT-qPCR analysis are shown in Table 1. Data were normalized to the expression of GAPDH using the $2^{-\Delta\Delta CT}$ method [1]. All the experiments were repeated three times.

Table 1. Sequences of the primers used for RT-qPCR to determine the mRNA levels of inflammatory factors in HLFS-RA cells

Genes	5'-3'	Sequences
GAPDH	Forward	CATGAGAAGTATGACAACAGCCT
	Reverse	AGTCCTTCCACGATACCAAAGT
IL-1β	Forward	TTCGACACATGGGATAACGAGG
	Reverse	TTTTTGCTGTGAGTCCCGGAG
IL-6	Forward	ACTCACCTCTTCAGAACGAATTG
	Reverse	CCATCTTTGGAAGGTTCAGGTTG
MMP-9	Forward	TGTACCGCTATGGTTACACTCG
	Reverse	GGCAGGGACAGTTGCTTCT
VEGF	Forward	AGGGCAGAATCATCACGAAGT
	Reverse	AGGGTCTCGATTGGATGGCA
Caspase3 (cleaved)	Forward	TTACAGTGAACACCTCTACCAATGCCCCA
	Reverse	TCCGTGAAAACACTAATCACCTTGCCCCA
Bax	Forward	GGGAGACACCTGAGCTGACC
	Reverse	GGACTCCAGCCACAAAGATGG
Bcl-2	Forward	GAACTGGGGGAGGATTGTGGCC
	Reverse	TCGACGTTTTGCCTGAAGACTGTTAA

Western blot determination of proteins related to the NF-κB pathway in HFLS-RA cells

HFLS-RA cells were cultured in 6-well plates for 12 h and then treated with TNF-α (10 ng/mL) and EF (400, 800, and 1600 μg/mL) for 24 h. RIPA lysate (including protease inhibitor and phosphatase inhibitor) was then used to lyse the cells. Protein concentrations were then determined with a BCA protein assay kit (Meilunbio, China). Equal concentrations of each protein lysate from each group were then mixed with loading buffer, separated by SDS-PAGE (EpiZyme, China), and then electro-transferred to nitrocellulose membranes. Next, membranes were blocked with 5% skimmed milk powder and incubated overnight with primary antibody at 4°C. The following morning, the membrane was incubated with secondary antibody at room temperature and immunoreactive bands were detected by enhanced chemiluminescence. The gray value of the protein bands was analyzed and the ratio of the target protein to GAPDH was used to evaluate the expression level of each protein. All the experiments were repeated three times.

Cell viability assays for RAW264.7 cells

RAW264.7 cells were purchased from Huatuo Biotechnology Co., Ltd. (Guangzhou, China). These cells were cultured as well as the HFLS-RA cells. Cell Counting Kit-8 (CCK-8) assay (Dojindo, Kunamoto, Japan) was used in accordance with the manufacturer's instructions, to determine cell viability. RAW264.7 cells were pre-incubated for 24 h with EF at various concentrations (0, 50, 100, 200, 400, 800, 1600 and 2000 μg/mL) in 96-well plates. Then, 10% CCK8 medium was added to the 96-well plates and a microplate reader was used to measure the absorbance at 450 nm. The relative rate of cell viability was expressed as a proportion (%) of the control group.

NO release in RAW264.7 cells

RAW264.7 cells were pre-incubated for 24 h with EF at various concentrations (0,, 50, 100, 200, 400, 800, 1600 and 2000 μg/mL) in 96-well plates. Then, suction the cell supernatant and Griess medium was added to the 96-well plates and a microplate reader was used to measure the absorbance at 540 nm. The relative NO release was expressed as a proportion (%) of the control group.

Trap stain

RAW264.7 cells were inoculated in 24-well plates. Next, 10% FBS + 1% penicillin and streptomycin + 50 ng/mL M-CSF + 50 ng/mL RANKL were used as the inducer in each group. The cells were pre-incubated with EF at various concentrations (400, 800, 1600 μg/ml) and induced for 7 days, the solution was changed every other day. Cells were stained with TRAP staining kit (Sigma, No.387) and observed microscopically. Red cells with more than three nuclei were assigned as osteoclasts.

Western blot determination of proteins related to the NF-κB pathway in RAW264.7 cells

RAW264.7 cells were inoculated in 24-well plates. Next, 10% FBS + 1% penicillin and streptomycin + 50 ng/mL M-CSF + 50 ng/mL RANKL were used as the inducer in each group. The cells were pre-incubated with EF at various concentrations (400, 800, 1600 μg/ml) and induced for 7 days, the solution was changed every other day. Then the cells were treated with TNF-α (10 ng/mL) for 24 h. Proteins were then separated and subject to western blotting as described previously in order to determine the

levels of proteins related to the NF-κB pathway. All the experiments were repeated three times.

Collagen II-induced arthritis in rats

The method for generating the CIA rat model was described previously (Wang et al.,2018). In brief, approximately 3 mg/mL of bovine type II collagen (CII) in 0.1 Macetic acid was emulsified with an equal volume of complete Freund's adjuvant (CFA) to create a stable CII/CFA emulsion (10 mg/mL). With the exception of the control group (6 rats), all rats were intradermally injected with the CII/ CFA emulsion in the back (0.1 mL) and tail (0.1 mL); the day of administration was referred to as day 0. On the 7th day, CIA rats received 0.1 mL of a CII/CFA booster via intradermal tail injection. After 14 days of modeling, the degree of posterior plantar redness and swelling of CIA rats was significantly different from that of blank control group according to the measurement of plantar volume and arthritis score ($P<0.05$), in line with the standard of arthritis model, indicating successful modeling (Wang et al.,2018, Xing et al.,2020). Then, the CIA rats were randomly divided into four groups with 6 rats per group. The control group and the model group were given 0.1 mL/100 g of distilled water; the other group was given EF at a dose of 2 $g \cdot kg^{-1} \cdot day^{-1}$ (EF-L) or 4 $g \cdot kg^{-1} \cdot day^{-1}$(EF-H). The positive control group was given methotrexate (MTX) at a dose of 0.3 $mg \cdot kg^{-1} \cdot day^{-1}$ (Wang et al., 2018). Dosing was carried out once a day for 4 weeks. At the beginning of day 0, we measured foot volume in each rat using a plantar volume meter; we also determined the arthritis score every 7 days until the end of the experiment. The flow chart of animal experiments is shown in Figure 1.

Micro-CT scanning

On the 42nd day, the rats were sacrificed and the right ankle joints were fixed in 4% paraformaldehyde (PFA). Next, we used high-resolution micro-CT (Skyscan 1176; Bruker, Billerica, MA, USA) to determine bone erosion in the distal thigh ankle joint. Then, we reconstructed a three-dimensional (3D) structure of the hind paws using Mimics 18.0 software (Materialise, Leuven, Belgium). We analyzed several bone morphometric parameters, including the proportion (%) of bone mineral density (BMD), bone volume/tissue volume (BV/TV), mean trabecular number (Tb.N), and mean trabecular separation (Tb.Sp).

Histopathological analysis

On the 42nd day, the rats were sacrificed and the left ankle joints were taken from each rat and fixed in 4% PFA. Fixed joints were then decalcified with 10% ethylenediamine tetra acetic acid (EDTA), paraffin-embedded, and then sliced into 4 mm slices with a microtome (Leica Microsystems, Wetzlar, Germany). Knee sections prepared from each group were then stained in hematoxylin and eosin (H&E). Pathological improvement in the ankle joints was then evaluated by examining the tissue sections and H&E staining. Synovial inflammation, angiogenesis, and bone destruction was then examined in the hind ankle joints and scored under a microscope. The scoring criteria have been reported previously [1]: 0 points = no inflammatory cell infiltration, pannus formation, or bone damage; 1 point = inflammatory cell infiltration or mild edema, a small amount of pannus formation; 2 points = moderate infiltration with pannus formation and moderate bone damage; 3 points = severe infiltration with moderate articular cavity stenosis; 4 points = pannus formation, severe bone damage.

SafraninO-fast green staining

Histological sections were prepared from the knees of all rats and then stained with the SafraninO-Fast Green Staining Kit (Solarbio, China). Pathological improvements in the ankle joint were then evaluated.

ELISA

On the 42nd day, the rats were sacrificed, and blood was taken from the abdominal aorta. Commercial ELISA kits were then used to assay the serum levels of IL-1β and TNF-α, in accordance with the manufacturer's protocol. Optical density was quantified at 450 nm using a microplate reader and serum concentrations of each factor were calculated by reference to a standard curve.

Determining the mRNA levels of inflammatory factors in the rat model of CIA

Rats were sacrificed on day 42 and the spleen and joints were removed from each group. RNA was extracted with EZ-press RNA Purification Kit and cDNA was synthesized by 4 × Reverse Transcription Master Mix. The primers used for RT-qPCR analysis are shown in Table 2. Data were normalized to the expression of GAPDH using the $2^{-\Delta\Delta CT}$ method [1]. All the experiments were repeated three times.

Table 2. Sequences of the primers used in RT-qPCR to determine the mRNA levels of inflammatory factors in the rat model of CIA.

Genes	5'-3'	Sequences
GAPDH	Forward	CCACCCATGGCAAATTCCATGGCA
	Reverse	TCTAGACGGCAGGTCAGGTCCACC
TNF-α	Forward	GGAAAGCATGATCCGAGATG
	Reverse	CGAGCAGGAATGAGAAGAGG
TRAF-6	Forward	TCTCGGAGTGCTGCGTGTATAGG
	Reverse	GTCGCTTAGAGACTGGCTGGAC
IL-1β	Forward	CTCACAGCATCTCGACAAGAG
	Reverse	CACACTAGCAGGTCGTCATCATCC
IL-17	Forward	GCCGAGGCCAATAACTTTCT
	Reverse	GAGTCCAGGGTGAAGTGGAA
CTSK	Forward	TAGCACCCTTAGTCTTCCGC
	Reverse	CTTGAACACCCACATCCTGC
NFATc-1	Forward	GGAGAGTCCGAGAATCGAGAT
	Reverse	TTGCAGCTAGGAAGTACGTCT
TRAP	Forward	TGGGTGACCTGGGATGGATT
	Reverse	AGCCACAAATCTCAGGGTGG
c-Fos	Forward	TTTCAACGCCGACTACGAGG
	Reverse	GCGCAAAAGTCCTGTGTGTT
RANKL	Forward	AGGCTGGGCCAAGATCTCTA

	Reverse	GATAGTCCGCAGGTACGCTC
VEGF	Forward	GGCAGCTTGAGTTAAACGAAC
	Reverse	TGGTGACATGGTTAATCGGTC
HIF-1	Forward	GGAAATGCTGGCTCCCTAT
	Reverse	CTGTAACTGGGTCTGCTGGA
TIMP-1	Forward	CGAGACCACCTTATACCAGCG
	Reverse	ATGACTGGGGTGTAGGCGTA
OPG	Forward	GGCAGGGCATACTTCCTGTT
	Reverse	GCCACTTGTTCATTGTGGTCC

Western blot determination of proteins related to the NF-κB pathway in the rat model of CIA

The rats in each group were all sacrificed on day 42. Taking each group as a unit, 20mg of pooled joint material was ground, and protein was extracted on ice with RPIA lysate (including protease inhibitor and phosphatase inhibitor). Proteins were then separated and subject to western blotting as described previously in order to determine the levels of proteins related to the NF-κB pathway.

Statistical analysis

All data were analyzed with SPSS version 26.0 software (SPSS Inc., Chicago, IL, USA). Data are expressed as mean ± standard error of the mean (SD). The significance of differences between groups was evaluated using the Student's t-test, $p < 0.05$ was considered to be statistically significant.

Results

EF inhibited the proliferation of TNF-α stimulated HFLS-RA cells

The influence of EF on HFLS-RA cell viability was investigated with the CCK-8 assay. As shown in Fig. 2A, EF was not cytotoxic at either 24 or 48 h. We investigated the effects of EF on the proliferation of TNF-α-stimulated HFLS-RA cells. Fig. 2B shows that EF (400, 800, 1600 μg/mL) was able to inhibit the proliferation of TNF-α stimulated HFLS-RA cells (*$p < 0.05$, **$p < 0.01$, ***$p < 0.001$). Furthermore, preliminary colony experiments showed that EF (400, 800, 1600 μg/mL) exhibited the best ability to inhibit proliferation (Fig. 2C and D) (*$p < 0.05$, ***$p < 0.001$); we therefore chose these concentrations of EF (400, 800, 1600 μg/mL) for subsequent experiments. EdU incorporation assays (Fig. 2E) showed that EF treatment (800, 1600 μg/mL) significantly blocked TNF-α-induced proliferation in HFLS-RA cells. Moreover, the anti-proliferative effect of EF occurred in a concentration-dependent manner.

EF inhibited cell migration and invasion in TNF-α stimulated HFLS-RA cells

Next, we evaluated the effects of EF on the migration and invasion of HFLS-RA cells. As shown in Fig. 3A and C, the scratch area in the EF group was significantly larger than that in the TNF-α group, thus indicating that the administration of EF inhibited the migration of cells (***$p < 0.001$). We also carried out an invasion assay to evaluate the effect of EF on the invasion of cells (Fig. 3B and D). We found that EF significantly inhibited cell invasion (**$p < 0.01$, ***$p < 0.001$).

EF induced apoptosis in TNF-α-stimulated HFLS-RA cells via the NF-κB pathway

Our previous results indicated that EF exhibited notable antiproliferative effects against HFLS-RA cells. In order to investigate the inhibitory effect of EF on the proliferation of HFLS-RA cells, we next investigated the ability of EF to induce apoptosis in HFLS-RA cells by performing flow cytometry and RT-qPCR. As shown in Fig. 4A and B, there was a gradual increase in apoptotic ratio as the concentration of EF increased (*$p < 0.05$, ***$p < 0.001$). As shown in Fig. 4C and D, the mRNA levels of *IL-1β*, *IL-6*, *VEGF*, and *MMP-9*, all decreased significantly with increased concentrations of EF (400, 800, 1600 μg/mL) when compared to the TNF-α group (*$p < 0.05$, **$p < 0.01$, ***$p < 0.001$). Compared with the TNF-α group, the mRNA levels of *Caspase3 (cleaved)* and *Bax* in the EF group were significantly higher, and the mRNA levels of *Bcl-2* in the EF group were significantly lower (**$p < 0.01$, ***$p < 0.001$). These data indicate that EF can induce apoptosis in HFLS-RA cells. To further explore the potential mechanism of EF inducing apoptosis of HFLS-RA cells, we measured the protein levels of factors related to the NF-κB pathway and found that(Fig. 5A,B), compared with the TNF-α group, the protein levels of p-Iκκ, p-IκB, and p-p65, were significantly reduced (**$p < 0.01$, ***$p < 0.001$). Consistent with RT-qPCR results, the protein levels of Caspase3 (cleaved) and Bax in the EF group were significantly higher, while the mRNA content of *Bcl-2* in the EF group were significantly lower(Fig. 5C,D). These results suggested that EF can induce apoptosis in HFLS-RA cells *via* the NF-κB pathway.

EF inhibited differentiation into osteoclasts in RANKL-stimulated RAW264.7 cells via the NF-κB pathway

Our previous results indicated that EF had a significant anti-proliferation effect on HFLS-RA cells and could induce apoptosis of HFLS cells. In order to investigate the effect of EF on the osteoclast differentiation of RAW264.7 cells, we next investigated the ability of EF on the osteoclast differentiation of RAW264.7 cells induced by RANKL by TRAP staining and Western blot. As shown in Fig. 6A, the influence of EF on RAW264.7 cell viability was investigated with the CCK-8 assay, EF was not cytotoxic at either 24h. We investigated the effects of EF on the proliferation of LPS-stimulated RAW264.7 cells. Fig. 6B shows that EF (1600, 2000 μg/mL) was able to inhibit the proliferation of LPS-stimulated RAW264.7 (**$p < 0.01$, ***$p < 0.001$). By TRAP staining and Western blot(Fig. 6C,D), we found that EF can inhibit the osteoclast differentiation of RAW264.7 cells induced by RANKL and inhibit the activation of NF-κB pathway (*$p < 0.05$, **$p < 0.01$, ***$p < 0.001$).

EF exhibits significant anti-arthritic effects in the rat model of CIA

To determine whether EF is able to exhibit inflammatory bone destruction effects on RA *in vivo*, we established a rat model of CIA. We initiated EF treatment on day 14 after successfully modeling. As shown in Fig. 7A, the CIA rats weighed significantly less than the normal group after modeling than the control group. Our data also showed that the CIA rats showed significant joint inflammation and that EF treatment reduced the severity of disease and joint swelling in the CIA rats (Fig. 7B and C) (**$p < 0.01$, ***$p < 0.001$). In addition, histological results showed that the ankle joints in CIA rats exhibited inflammatory cell infiltration in the soft tissue and the lining of the synovial layer. Data also revealed cartilage destruction which led to pannus formation and narrowing in the joint space (Fig. 7D and E). EF treatment attenuated joint inflammation by reducing synovial inflammatory cell infiltration and reducing pannus formation in the CIA rats. SafraninO-Fast Green Staining also showed that EF reduced cartilage damage in RA (Fig. 7F).

The effect of EF on bone destruction

Because EF treatment had a positive effect on pathological bone destruction, we next explored the potential of EF to reduce bone loss; we did this by carrying out morphological analysis and creating a three-dimensional reconstruction of the tibia and

ankle (Fig. 8A and B). We found that BMD and BV/TV were significantly reduced ($p < 0.001$). There was also a reduction in the quantity of bone trabecula, although this was not statistically significant. There was a significant increase in the separating degree of the Tb.Sp ($p < 0.001$). In contrast, a high dose of EF partially prevented the sharp decline in bone mass and the deterioration of trabecular microstructures in CIA rats. However, there were no significant differences when low-dose EF treatments were compared to controls.

The effect of EF on the expression of bone metabolic indices in serum and spleen

CTX-1, ICTP, PINP, and BGP, are commonly used as clinical markers for the detection of osteoporosis. Increases and decreases in these factors can reflect the status of bone destruction. The serum levels of CTX-1 and ICTP, and the mRNA levels of *TNF-α*, *TRAF-6*, *IL-1β*, and *IL-17*, in the spleen of the CIA group were significantly increased than the control group. Serum levels of PINP and BGP in the CIA group were significantly lower in the CIA group than in the controls (Fig. 9) (#$p < 0.05$, ##$p < 0.01$, ###$p < 0.001$). Following EF administration, the levels of CTX-1 and ICTP, and the mRNA levels of TNF-α, TRAF-6, IL-1β, and IL-17, in the spleen were significantly lower than those in the CIA group; serum levels of PINP and BGP were also significantly higher than in the controls (*$p < 0.05$, **$p < 0.01$, ***$p < 0.001$). In addition, EF reduced the levels of inflammatory factors in the spleen and regulated metabolic events in the bone; this was consistent with the micro-CT results and suggested that EF has a certain regulatory effect on damage caused by osteoarthritis.

The effect of EF on bone metabolic indices in joint tissue

RANKL, c-FOS, NFATc1, CTSK, and TRAP, are all considered as markers for the production of osteoclasts; VEGF and HIF-1 are also considered to be related to angiogenesis. Increased levels of these factors are considered to be indicators of bone damage. As shown in Fig. 10, compared to the normal group, the levels of these factors were significantly higher in the CIA group, but significantly lower in the EF group than in the CIA group (*$p < 0.05$, **$p < 0.01$, ***$p < 0.001$). TIMP-1 is the inhibitory factor for MMP-9 (a biomarker for the local inflammation of joints and is known to be related to bone destruction). The levels of TIMP-1 and OPG in the EF group were significantly increased than the CIA group. Collectively, these data showed that EF can improve the osteoarthritic regulation of bone metabolism at the genetic level.

The effect of EF on the NF-κB pathway in joint tissue

Next, as shown in Fig. 11, we further explored the potential mechanism underlying the effects of EF on the CIA rat. We measured the protein levels of key factors in the NF-κB pathway and found that, compared with the CIA group, the protein levels of p-Iκκ, p-IκB, and p-p65, were significantly lower in the EF group (*$p < 0.05$, **$p < 0.01$, ***$p < 0.001$). These results suggested that EF could improve joint inflammation and bone destruction by inhibiting activation of the NF-κB pathway.

Chemical profiles of the ethanol extract of male flower of *Eucommia ulmoides Oliv.*

HPLC chromatogram of chemical constituents in the ethanol extract of male flower of *Eucommia ulmoides Oliv.* As shown in Fig. 12. Consequently, the 3 main constituents peaks were identified as geniposidic acid (4.3 mg/g), chlorogenic acid (1.5 mg/g), quercetin (0.2 mg/g).

Discussion

RA is a chronic and systemic autoimmune disease that is mainly characterized by the proliferation of synovial cells and bone destruction. The pathogenesis of RA is complex; the main pathological features are synovial cell proliferation and the destruction of cartilage and bone. Collectively, these processes can cause a significant amount of pain and can adversely affect the quality of life [12]. Joint symptoms can be divided into two types: synovial inflammation and joint structure destruction. Once bone has begun to undergo degeneration, it is very difficult to stop or reverse this process [1]. Our current data show that EF can significantly reduce the degree of joint swelling in a rat model of CIA. Pathological sections further showed that EF can reduce partial necrosis of the articular cartilage, reduce pannus formation, fibrous tissue changes, and synovium hyperplasia. Micro-CT scans showed significant improvement in bone destruction in the group of CIA rats treated with EF. These results suggest that EF can effectively inhibit the bone destruction experienced by joints in the rat model of CIA and improve pathological changes within the joints.

Activated macrophages play an important role in the occurrence, maintenance, and pathogenesis, of RA by secreting pro-inflammatory factors, including TNF-α. HFLS-RA synovial cells are commonly used in the study of RA. When joint inflammation occurs, TNF-α levels are known to increase significantly. Synovial cells also proliferate and invade the cartilage and bone, thus leading to pannus formation. The excessive proliferation and inadequate apoptosis of RA-FLS is generally recognized as the pathological basis of RA. There is increasing evidence to support the fact that regulating the activation of HFLS-RA migration and invasion may represent a new treatment strategy to prevent the destruction of RA joints [13]. It has also been reported that FLS in RA patients are resistant to apoptosis due to an imbalance of anti- and pro-apoptotic molecules (such as Caspase3 (cleaved) and Bax) and that anti-apoptotic mediators may play a key role, including Bcl-2 [14]. In addition, HFLS-RA also showed high proliferative behavior similar to tumor cells, so we conducted proliferation experiments [15]. In the present study, we used TNF-α to stimulate HFLS-RA cells. We found that EF inhibited synovial cell proliferation in both colony and EdU experiments. EF also promoted the apoptosis of synovitis cells, as determined by flow cytometry. RT-qPCR and WB experiments further demonstrated that the levels of p-p65 NF-κB, p-Iκκαβ, and p-IκBα, proteins were significantly reduced treated with EF. The increased levels of Caspase3 and Bax, and decreased levels of Bcl-2, demonstrated that EF could promote apoptosis by inhibiting activation of the NF-κB pathway. In addition, we found that EF could significantly inhibit the release of NO in LPS-induced RAW264.7 cells without cytotoxicity. Therefore, we further induced RAW264.7 cells with RANKL and M-CSF, and found that EF could significantly inhibit the differentiation of RAW264.7 cell into osteoclasts and inhibit the activation of NF-κB pathway in osteoclasts. Therefore, we speculated that the effect of EF on the improvement of bone destruction may relate to the inhibition of NF-κB pathway activation and osteoclast generation.

In addition, RA-FLS causes an increase in the expression levels of matrix metalloproteinases (MMPs), increases the rate of degradation in the cartilage extracellular matrix, migration and invasion of cartilage and bone, and causes infiltration and destruction of the joint [15]. Some studies have found that the intensification of bone resorption is a major factor of joint destruction in rheumatoid arthritis, and the increase of CTX-1 in serum is closely related to bone resorption [16]. Therefore, several factors related to bone resorption and bone formation were measured in this experiment, such as CTX-1、ICTP、PINP and BGP. In the study, we found that EF reduced the levels of CTX-1 and ICTP but increased the levels of PINP and BGP in the serum of rats. TNF-α, IL-1 and IL-6 stimulates neutrophil migration, promotes osteoclast maturation, and promotes the secretion of VEGF, thus leading to the destruction of joints [17]. In the present study, EF reduced the levels of several factors in the spleen of CIA rats, including TNF-α, TRAF-6, IL-1β, and IL-17. We also found that the expression levels of VEGF and HIF-1, along with angiogenesis-related factors in the cartilage joints of rats, were significantly reduced in pathological tissue sections.

The NF-κB signaling pathway is associated with angiogenesis in RA. The increase in VEGF that is induced by nuclear factor-κB ligand receptor activator (RANKL) is mediated by nuclear factor-κB in osteoclasts [17]. Osteoclasts are the only cells that are capable of absorbing bone in the body. Bone resorption is achieved by close interaction with extracellular matrix proteins.

In RA, RANKL activates NF-κB signaling, and matrix enzymes that are synthesized by the osteoclasts, including histoprotease K (CTSK), cell oncogene c-FOS, and tartaric acid phosphatase 5 (TRAP). Collectively, these factors degrade bone matrix and exacerbate bone erosion [18]. RANKL signaling, acts *via* its receptor activator, NF-κB (RANK), and plays an important osteoclastic role in bone remodeling [19]. In the CIA group of rats, we observed a significant increase in the levels of osteoclast markers, including TRAP, NFATc1, CTSK, c-FOS, and RANKL, thus indicating that CIA rats exhibited significant levels of bone destruction; collectively, these factors had induced severe corrosion in the cartilage and bone tissue. Following administration, EF significantly reduced the mRNA levels of *TRAP*, *NFATc1*, *CTSK*, *c-FOS*, *RANKL*. The mRNA levels of OPG, a marker of osteogenesis, were significantly higher in the EF group, although this showed some variation. The MMP family is involved in tissue remodeling, repair, and angiogenesis, and is regulated by tissue metalloproteinase inhibitor (TIMP). In the event of osteoarthritis and RA, the family of MMP proteins is up-regulated and the balance with TIMP is destroyed [20]. In this study, we observed reduced levels of TIMP1 in the cartilage of rats in the model group. In contrast, levels of TIMP1 in the EF group increased to varying degrees, thus indicating that EF has the ability to improve arthritis. However, whether EF exerts impact on the family of MMP proteins requires further study. This study provides an experimental basis for the application of EF, but there are still many limitations. It is mainly limited to research design, such as clarifying the effect between active single component of TCM and active single component of TCM, the role of active single component of TCM in active single component of TCM, the main target of TCM, improving the method of in vitro study of TCM extract, etc. On the basis of this experiment, this research group will continue to search for active monomer components of Chinese medicine and further study its target mechanism.

In summary, the expression levels of p-p65 NF-κB, p-Iκκαβ, and p-IκBα, in the cartilage of the model group were significantly up-regulated. After treatment, the expression levels of p-p65 NF-κB, p-Iκκαβ, and p-IκBα, in the EF group were significantly reduced. These data demonstrate that EF may improve bone destruction in the rat model of CIA by inhibiting the NF-κB signaling pathway.

Conclusion

EF inhibits synovial cell proliferation, promotes apoptosis and inhibits osteoclast differentiation by inhibiting activation of the NF-κB pathway. EF also reduces toes swelling in the rat model of CIA, inhibits the expression of pro-angiogenic factors, and delays the destruction of articular cartilage and bone. The mechanism underlying the effects of EF is related to bone metabolism induced by the NF-κB pathway. We hope that the results of our study will help to elucidate the precise pharmacological mechanisms underlying the actions of EF and provide an experimental basis for the application of EF in the clinical treatment of RA.

Abbreviations

Bax, bcl-2-associated X protein; Bcl-2, b-cell lymphoma-2; Caspase3(cleaved), cysteinyl aspartate specific proteinase-3; CTSK, cathepsin K; EF, the male flower of Eucommia ulmoides Oliv.; HIF-1, hypoxia inducible factor-1; IL-17, interleukin-17; IL-1β, interleukin-1β; IL-6, interleukin-6; MMP-9, matrix metalloprotein-9; NFATc-1, nuclear factor; OPG, osteoprotegerin; RA, rheumatoid arthritis; RANKL, receptor activator of nuclear factor-κB ligand; TIMP-1, tissue inhibitor of metalloproteinases-1;TRAF-6, TNF receptor-associated factor-6; TRAP, tartrate resistant acid phosphatase; TNF-α, tumor necrosis factor; VEGF, vascular endothelial growth factor

Acknowledgments

We would like to thank The Charlesworth Group for their assistance with English language editing.

Author's contributions

Yan Zhang and Jian-Ying Wang wrote the paper; Hao Wang, Xiao-Yun Chend and Lei Zhang designed the experiments; Ying Yuan revised the article critically for important intellectual content. All authors approved the final version of the manuscript. All authors read and approved the final manuscript.

Funding

This research was supported by grants from the Natural Science Foundation of China (Reference: 81773922) and the Shanghai Natural Science Foundation (Reference: 19ZR1452000).

Availability of data and materials

The datasets used and/or analysed during the current study are available from the corresponding author on reasonable request.

Declarations

Ethics approval and consent to participate

This study was approved by the Committee on Ethical Use of Animals of Shanghai University of Traditional Chinese Medicine(Approval number: PZSHUTCM18122823)..

Consent for publication

Not applicable.

Competing interests

The authors declare that they have no competing interests.

Conflict of interest

The author states that there is no conflict of interest.

References

[1] Wang JY, Chen XJ, Zhang L, Pan YY, Gu ZX, He SM, Song ZP, Yuan Y. Comparative Studies of Different Extracts from Eucommia ulmoides Oliv. against Rheumatoid Arthritis in CIA Rats. Evid Based Complement Alternat Med. 2018;2018:7379893. https://doi.org/10.1155/2018/7379893

[2] Zhang Q, Liu J, Zhang M, Wei S, Li R, Gao Y, Peng W, Wu C. Apoptosis Induction of Fibroblast-Like Synoviocytes Is an Important Molecular-Mechanism for Herbal Medicine along with its Active Components in Treating Rheumatoid Arthritis. Biomolecules. Biomolecules. 2019;9(12):795. https://doi.org/10.3390/biom9120795.

[3] Jimi E, Fei H, Nakatomi C. NF-κB Signaling Regulates Physiological and Pathological Chondrogenesis. Int J Mol Sci. 2019;20(24):6275. https://doi.org/10.3390/ijms20246275

[4] Wu WY, Hou JJ, Long HL, Yang WZ, Liang J, Guo DA. TCM-based new drug discovery and development in China. Chin J Nat Med. 2014;12(4):241-250. https://doi.org/10.1016/S1875-5364(14)60050-9

[5] Daily JW, Zhang T, Cao S, Park S. Efficacy and Safety of GuiZhi-ShaoYao-ZhiMu Decoction for Treating Rheumatoid Arthritis: A Systematic Review and Meta-Analysis of Randomized Clinical Trials. J Altern Complement Med. 2017;23(10):756-770. https://doi.org/10.1089/acm.2017.0098

[6] Li ZY, Gu J, Yan J, Wang JJ, Huang WH, Tan ZR, Zhou G, Chen Y, Zhou HH, Ouyang DS. Hypertensive cardiac remodeling effects of lignan extracts from Eucommia ulmoides Oliv. bark--a famous traditional Chinese medicine. Am J

Chin Med. 2013;41(4):801-815. https://doi.org/10.1142/S0192415X13500547
[7] He X, Wang J, Li M, Hao D, Yang Y, Zhang C, He R, Tao R. Eucommia ulmoides Oliv.: ethnopharmacology, phytochemistry and pharmacology of an important traditional Chinese medicine. J Ethnopharmacol. 2014;151(1):78-92.
[8] Wang JY, Yuan Y, Chen XJ, Fu SG, Zhang L, Hong YL, You SF, Yang YQ. Extract from Eucommia ulmoides Oliv. ameliorates arthritis via regulation of inflammation, synoviocyte proliferation and osteoclastogenesis in vitro and in vivo. J Ethnopharmacol. 2016;194:609-616. https://doi.org/10.1016/j.jep.2016.10.038
[9] Chen XY, Wang FC, Yuan Y, Zhang L, Li XD, Jin SA, He SM, Wang JY, Comparative study of bark, leaf and male flower of Eucommia on pharmacodynamics. Journal of Gansu University of Chinese Medicine. 2016;33(05):5-8. https://doi.org/10.16841/j.issn1003-8450.2016.05.02
[10] Wang JY, Chen XJ, Zhang L, Pan YY, Gu ZX, Yuan Y. Anti-inflammatory effects of Eucommia ulmoides Oliv. male flower extract on lipopolysaccharide-induced inflammation. Chin Med J (Engl). 2019;132(3):319-328. https://doi.org/10.1097/CM9.0000000000000066
[11] Xing YY, Wang JY, Wang K, Zhang Y, Liu K, Chen XY, Yuan Y. Inhibition of Rheumatoid Arthritis Using Bark, Leaf, and Male Flower Extracts of Eucommia ulmoides. Evid Based Complement Alternat Med. 2020;2020:3260278. https://doi.org/10.1155/2020/3260278
[12] Zhao H, Lu A, He X. Roles of MicroRNAs in Bone Destruction of Rheumatoid Arthritis. Front Cell Dev Biol. 2020;8:600867. https://doi.org/10.3389/fcell.2020.600867
[13] Xu S, Xiao Y, Zeng S, Zou Y, Qiu Q, Huang M, Zhan Z, Liang L, Yang X, Xu H. Piperlongumine inhibits the proliferation, migration and invasion of fibroblast-like synoviocytes from patients with rheumatoid arthritis. Inflamm Res. 2018;67(3):233-243. https://doi.org/10.1007/s00011-017-1112-9
[14] Zhang Q, Peng W, Wei S, Wei D, Li R, Liu J, Peng L, Yang S, Gao Y, Wu C, Pu X. Guizhi-Shaoyao-Zhimu decoction possesses anti-arthritic effects on type II collagen-induced arthritis in rats via suppression of inflammatory reactions, inhibition of invasion & migration and induction of apoptosis in synovial fibroblasts. Biomed Pharmacother. 2019;118:109367. https://doi.org/10.1016/j.biopha.2019.109367
[15] Lin J, Yu Y, Wang X, Ke Y, Sun C, Yue L, Xu G, Xu B, Xu L, Cao H, Xu D, Olsen N, Chen W. Iguratimod Inhibits the Aggressiveness of Rheumatoid Fibroblast-Like Synoviocytes. J Immunol Res. 2019;2019:6929286. https://doi.org/10.1155/2019/6929286
[16] Engelmann R, Wang N, Kneitz C, Müller-Hilke B. Bone resorption correlates with the frequency of $CD5^+$ B cells in the blood of patients with rheumatoid arthritis. Rheumatology (Oxford). 2015;54(3):545-553. https://doi.org/10.1093/rheumatology/keu351
[17] Pirmardvand Chegini S, Varshosaz J, Taymouri S. Recent approaches for targeted drug delivery in rheumatoid arthritis diagnosis and treatment. Artif Cells Nanomed Biotechnol. 2018;46(sup2):502-514. https://doi.org/10.1080/21691401.2018.1460373
[18] Schett G, Gravallese E. Bone erosion in rheumatoid arthritis: mechanisms, diagnosis and treatment. Nat Rev Rheumatol. 2012;8(11):656-664. https://doi.org/10.1038/nrrheum.2012.153
[19] Ikebuchi Y, Aoki S, Honma M, Hayashi M, Sugamori Y, Khan M, Kariya Y, Kato G, Tabata Y, Penninger JM, Udagawa N, Aoki K, Suzuki H. Coupling of bone resorption and formation by RANKL reverse signalling. Nature. 2018;561(7722):195-200. https://doi.org/10.1038/s41586-018-0482-7
[20] Li X, Wu JF. Recent developments in patent anti-cancer agents targeting the matrix metalloproteinases (MMPs). Recent Pat Anticancer Drug Discov. 2010;5(2):109-141. https://doi.org/10.2174/157489210790936234

Figures

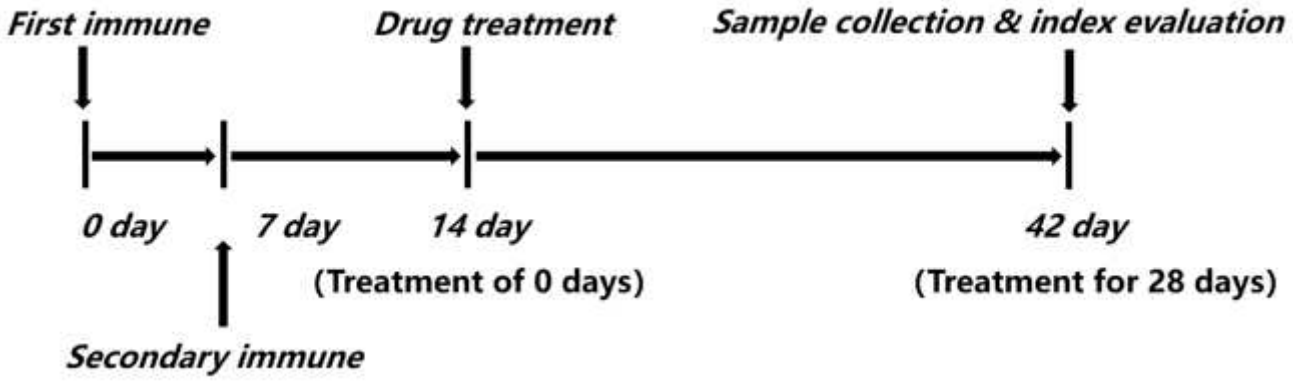

Figure 1

Flowchart of Animal Experiment.

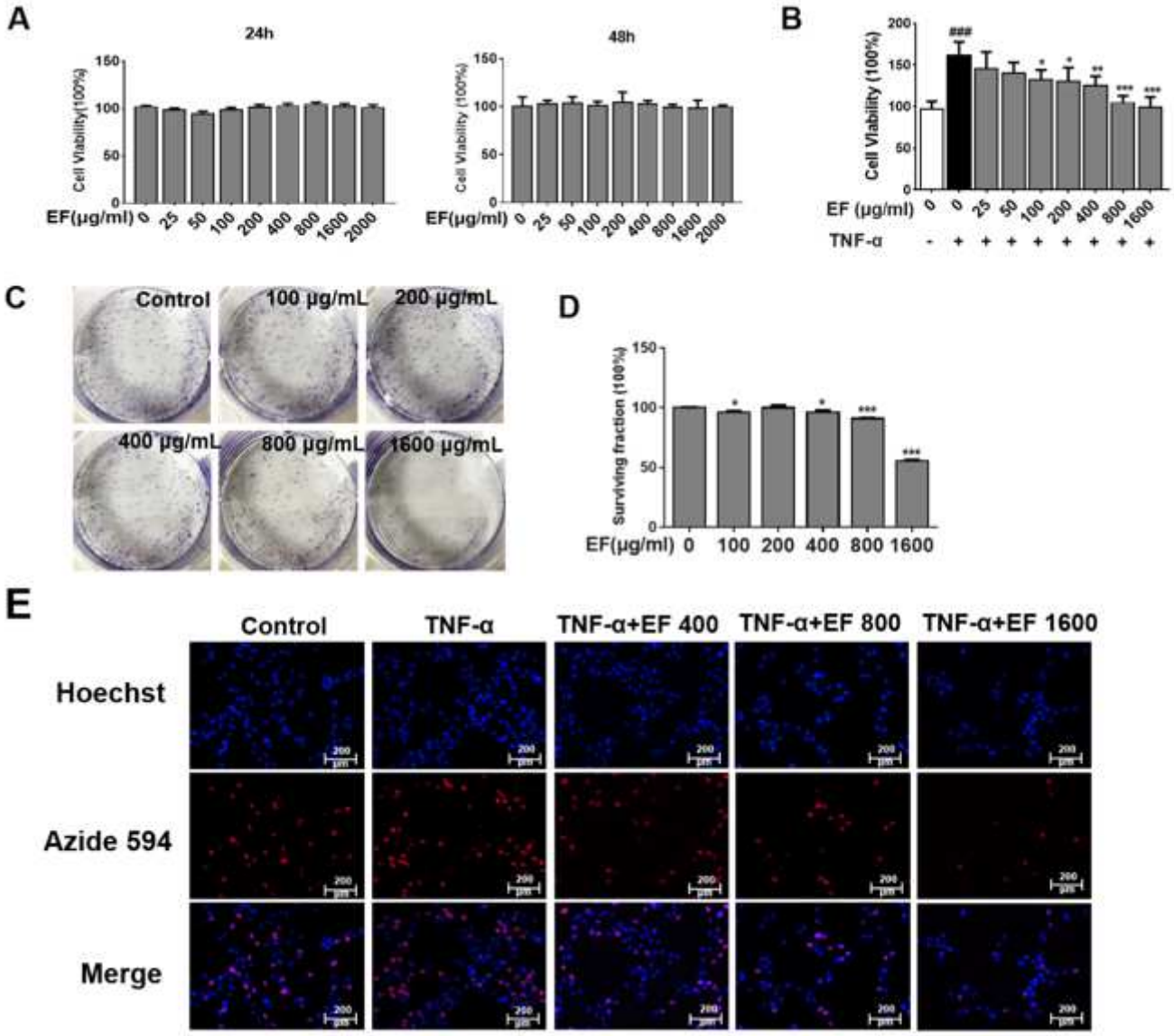

Figure 2

The effects of EF on the proliferation of HFLS-RA cells with and without TNF-α stimulation. (A) The cytotoxicity of EF in cultured cells was tested for 24 h and 48 h. (B) The anti-proliferative effects of EF against TNF-α stimulated HFLS-RA cells exhibited a concentration-dependent relationship). HFLS-RA cells were incubated with TNF-α (10 ng/mL) and EF (25, 50, 100, 200, 400, 800 and 1600 μg/mL) for 24 h. We then used the CCK-8 assay to determine the extent to which cell proliferation was inhibited (%). Data are represented as mean ± SD (n = 4), *p < 0.05, **p < 0.01, ***p < 0.001, vs. TNF-α cells (HFLS-RA cells treated by TNF-α alone). #p < 0.05, ##p < 0.01, ###p < 0.001, vs. Control cells. (C) A cell colony assay was used to investigate the effect of EF on the proliferation of HFLS-RA cells. (D) Data are represented as mean ± SD (n = 4), *p < 0.05, **p < 0.01, ***p < 0.001, vs. control cells. (E) HFLS-RA cells were seeded onto glass coverslips, starved, and then stimulated for 24 h with TNF-α (10 ng/mL) or EF (400, 800 and 1600 μg/mL). Cells were then stained with the EdU Cell Proliferation Kit .Hoechst (blue) and Azide594 (red) and visualized by fluorescence microscopy (200×).

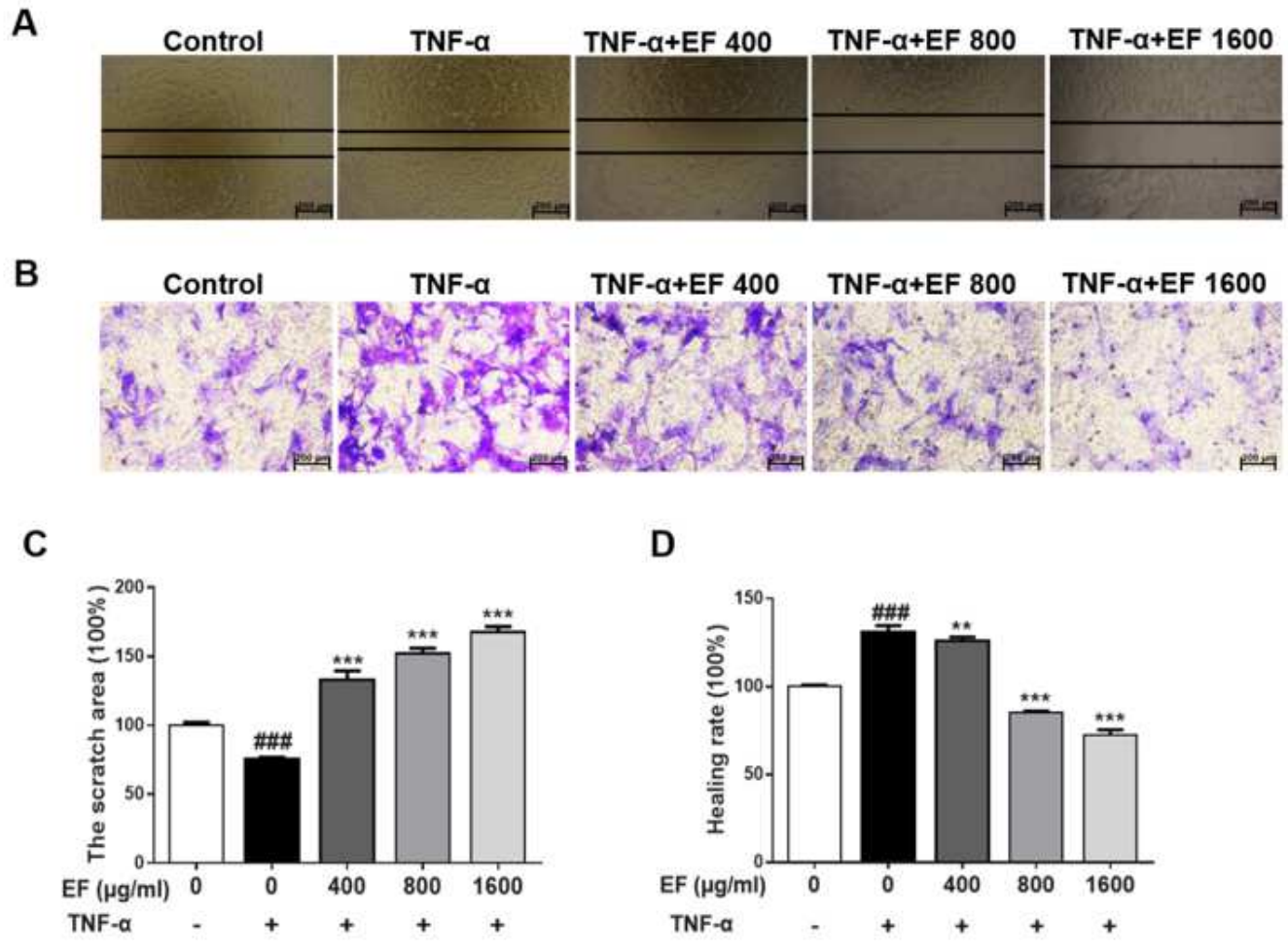

Figure 3

The effects of EF on the migration and invasion of TNF-α-stimulated HFLS-RA cells. Cells were incubated with EF (400, 800 and 1600 μg/mL) and TNF-α (10 ng/mL) for 24 h. (A, C) The effect of EF on HFLS-RA

cells (100×) with regard to wound migration. Cell mobility was calculated and photographed. (B, D) The invasion assay was carried out in a Matrigel basement membrane matrix chamber and invading cells were counted in order to quantify chemotaxis. Images show the invasion of HFLS-RA cells following EF treatment. Data are represented as mean ± SD (n = 4), *p < 0.05, **p < 0.01, ***p < 0.001, vs. TNF-α cells (HFLS-RA cells treated by TNF-α alone). #p < 0.05, ##p < 0.01, ###p < 0.001, vs. control cells.

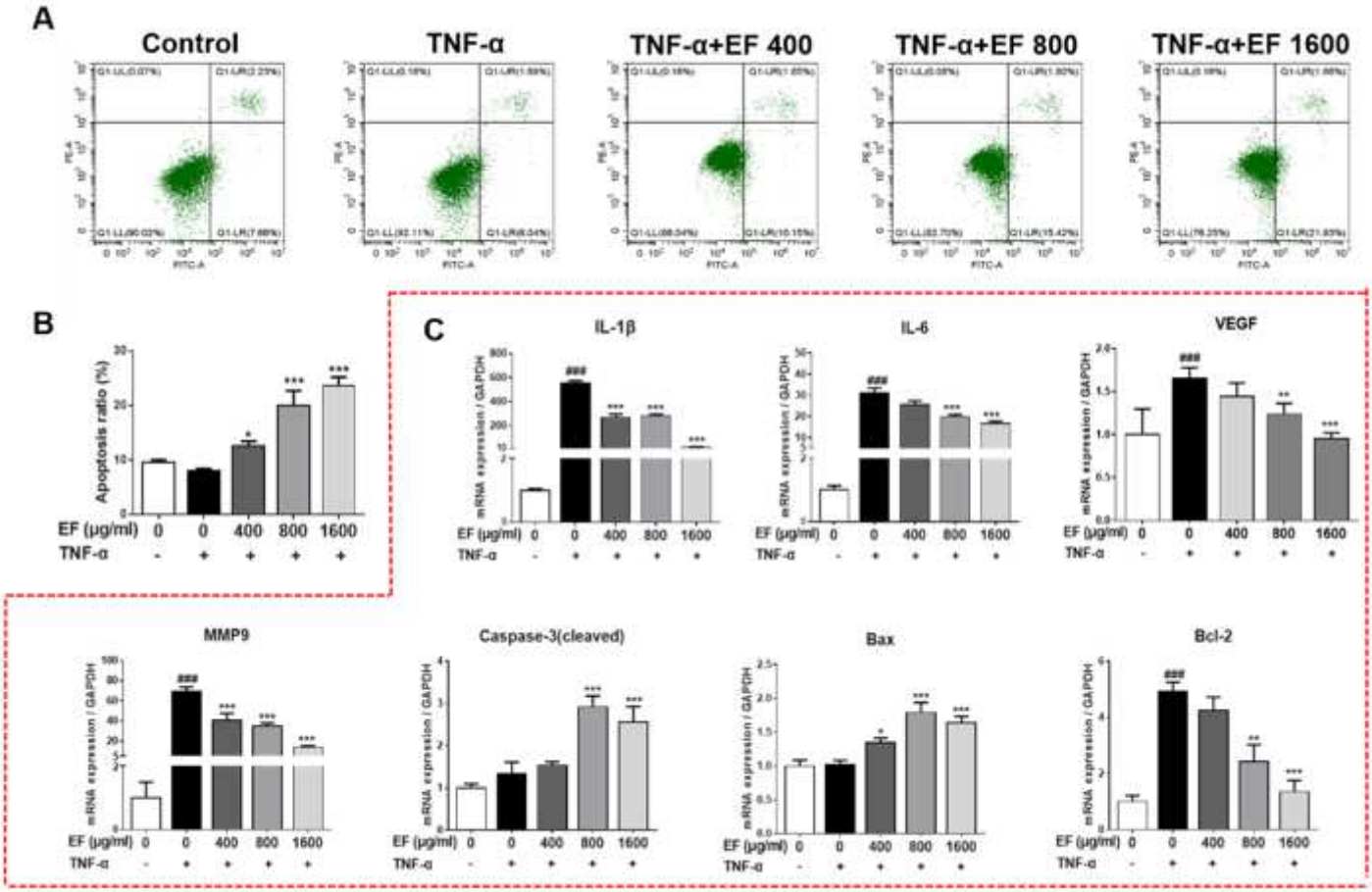

Figure 4

The apoptosis-inducing effects of EF in TNF-α-stimulated HFLS-RA cells. HFLS-RA cells were incubated with TNF-α (10 ng/mL) and EF (400, 800 and 1600 μg/mL) for 24 h. (A) Levels of apoptosis as determined by flow cytometry. Apoptotic cells were detected by staining with Annexin V-FITC/PI followed by flow cytometry. (B) Data are represented as mean ± SD (n = 4), *p < 0.05, **p < 0.01, ***p < 0.001, vs. TNF-α cells (HFLS-RA cells treated by TNF-α alone). #p < 0.05, ##p < 0.01, ###p < 0.001, vs. Control cells. (C) mRNA levels of IL-1β, IL-6, VEGF, MMP-9, Caspase-3, Bax, and Bcl-2, were determined by RT-qPCR. Data are represented as mean ± SD (n = 4), *p < 0.05, **p < 0.01, ***p < 0.001, vs. TNF-α cells (HFLS-RA cells treated by TNF-α alone). #p < 0.05, ##p < 0.01, ###p < 0.001, vs. control cells.

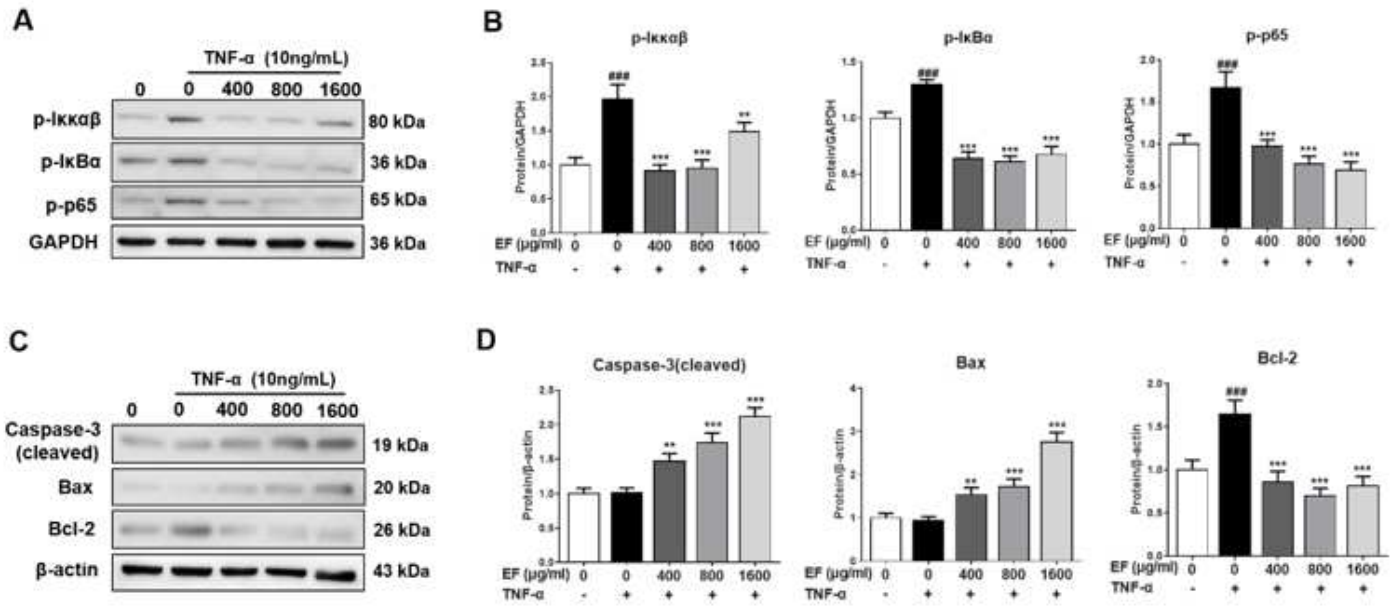

Figure 5

EF induced apoptosis in TNF-α stimulated HFLS-RA cells via the NF-κB pathway. HFLS-RA cells were incubated with TNF-α (10 ng/mL) and EF (400, 800 and 1600 μg/mL) for 24 h. (A, C) Western blot analysis was then conducted to determine the protein levels of p-p65 NF-κB, p-Ikkαβ, p-IκBα, Caspase3(cleaved)Bax, and Bcl-2. The effect of EF on the surface expression of TNF-α receptors on HFLS-RA cells. (B, D) Data are represented as mean ± SD (n = 3), *p < 0.05, **p < 0.01, ***p < 0.001, vs. TNF-α cells (HFLS-RA cells treated by TNF-α alone). #p < 0.05, ##p < 0.01, ###p < 0.001, vs. control cells.

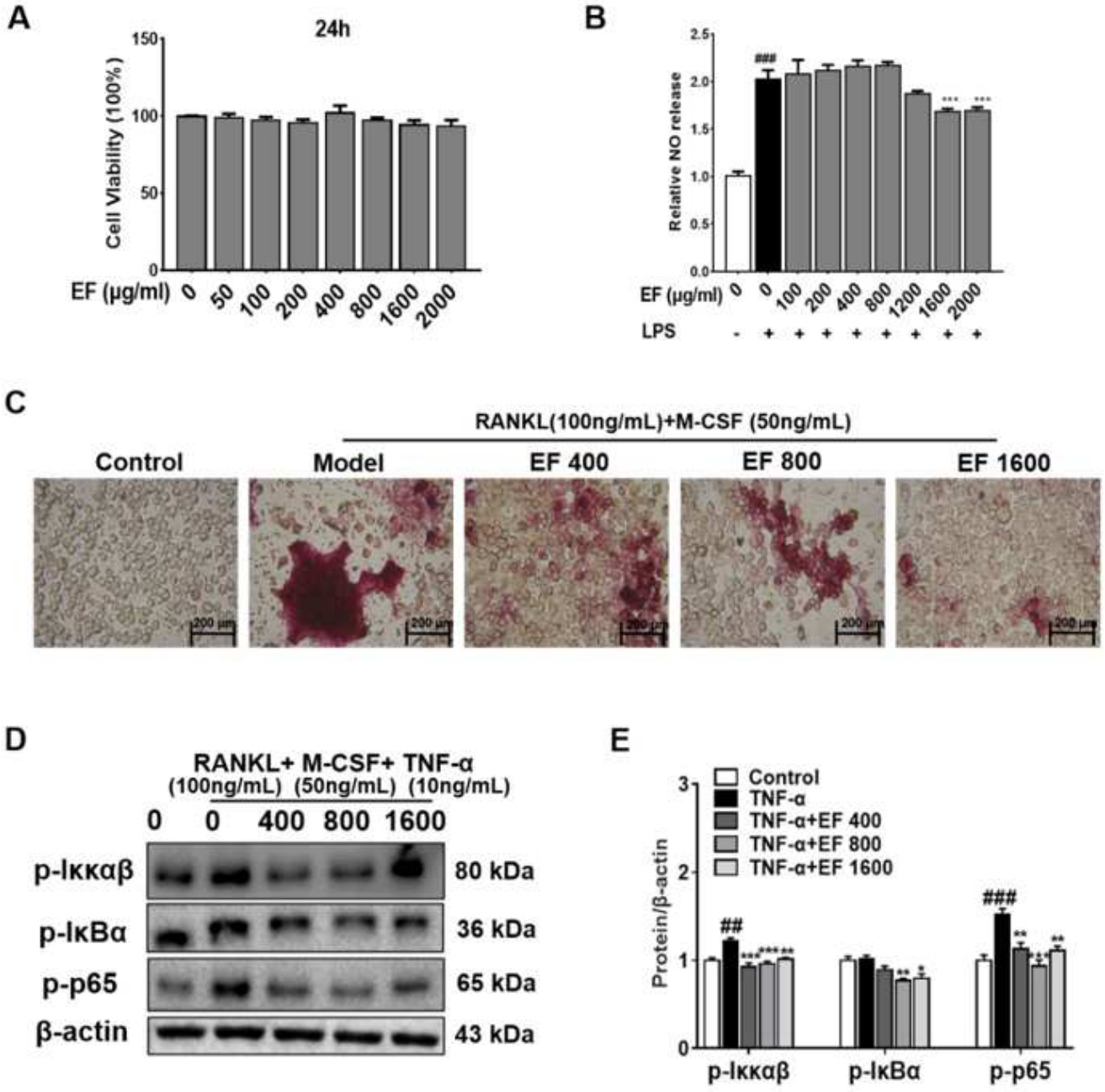

Figure 6

EF inhibited differentiation into osteoclasts in RANKL-stimulated RAW264.7 cells via the NF-κB pathway. (A) The cytotoxicity of EF in cultured cells was tested for 24 h . (B) RAW264.7 cells were incubated with LPS (1 μg/mL) and EF (100, 200, 400, 800, 1600, 2000 μg/mL) for 24 h. (C) TRAP staining assay was used to investigate the effect of EF on the differentiation into osteoclasts of RAW264.7 cells. (D) Western blot analysis was then conducted to determine the protein levels of p-p65 NF-κB, p-Iκκαβ, p-IκBα. (E) Data are represented as mean ± SD (n = 3), *p < 0.05, **p < 0.01, ***p < 0.001, vs. TNF-α cells . #p < 0.05, ##p < 0.01, ###p < 0.001, vs. control cells.

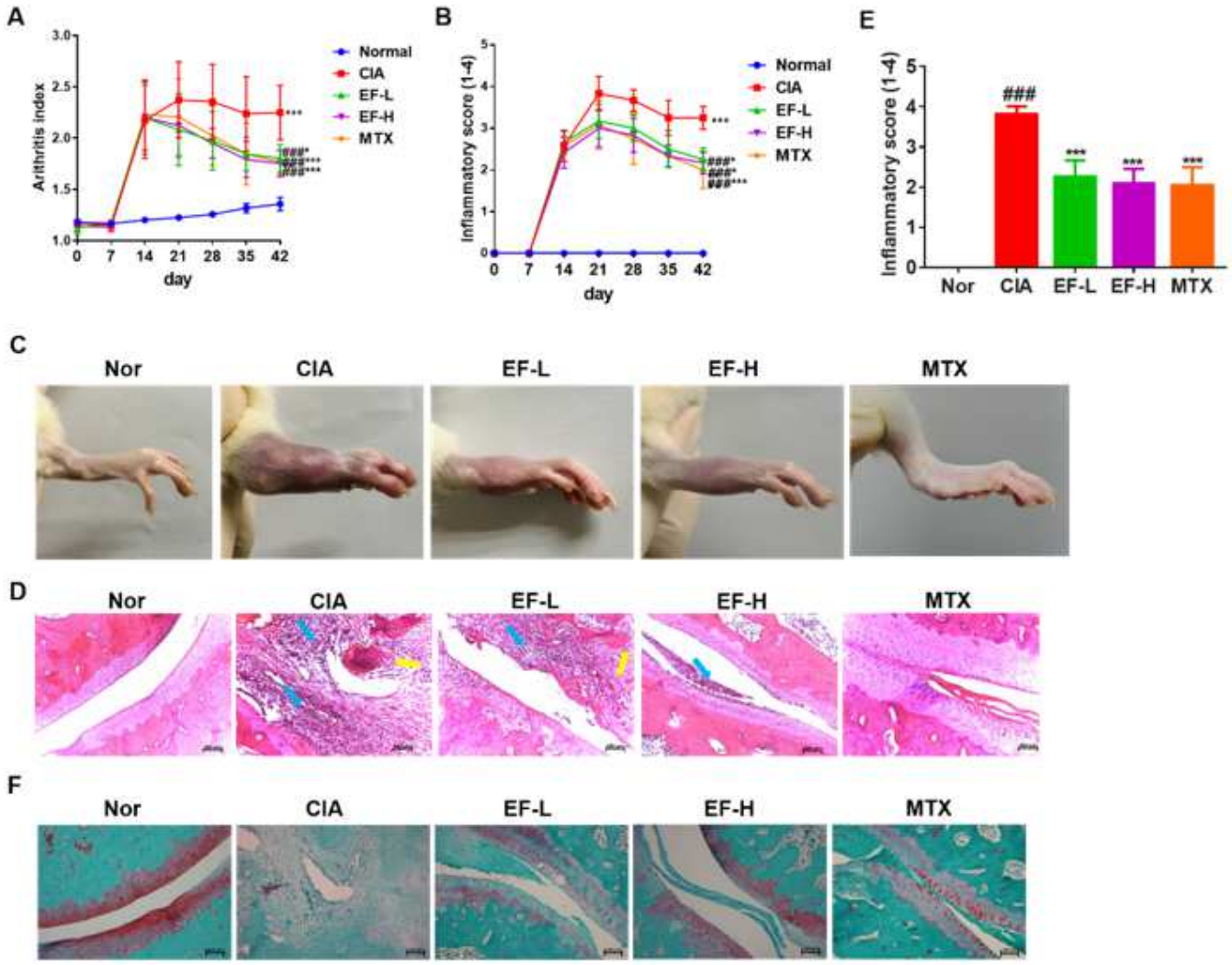

Figure 7

The anti-arthritic effects of EF on CIA rats. (A, B) The effects of EF on paw volume and arthritis score changes in CIA rats. (C) A typical paw of rats in different treatment groups. (D, E) Tissue sections of ankle joints stained with Hematoxylin and Eosin (HE). Blue arrow represents hyperplasia in the synovial membrane and pannus; the yellow arrow shows cartilage injury. (F) Tissue sections of ankle joints stained with SafraninO-Fast Green Staining. Data are represented as mean ± SD (n = 6), *p < 0.05, **p < 0.01, ***p < 0.001, vs. CIA animal (CIA rats without treatment by EF and MTX), #p < 0.05, ##p < 0.01, ###p < 0.001, vs. normal group.

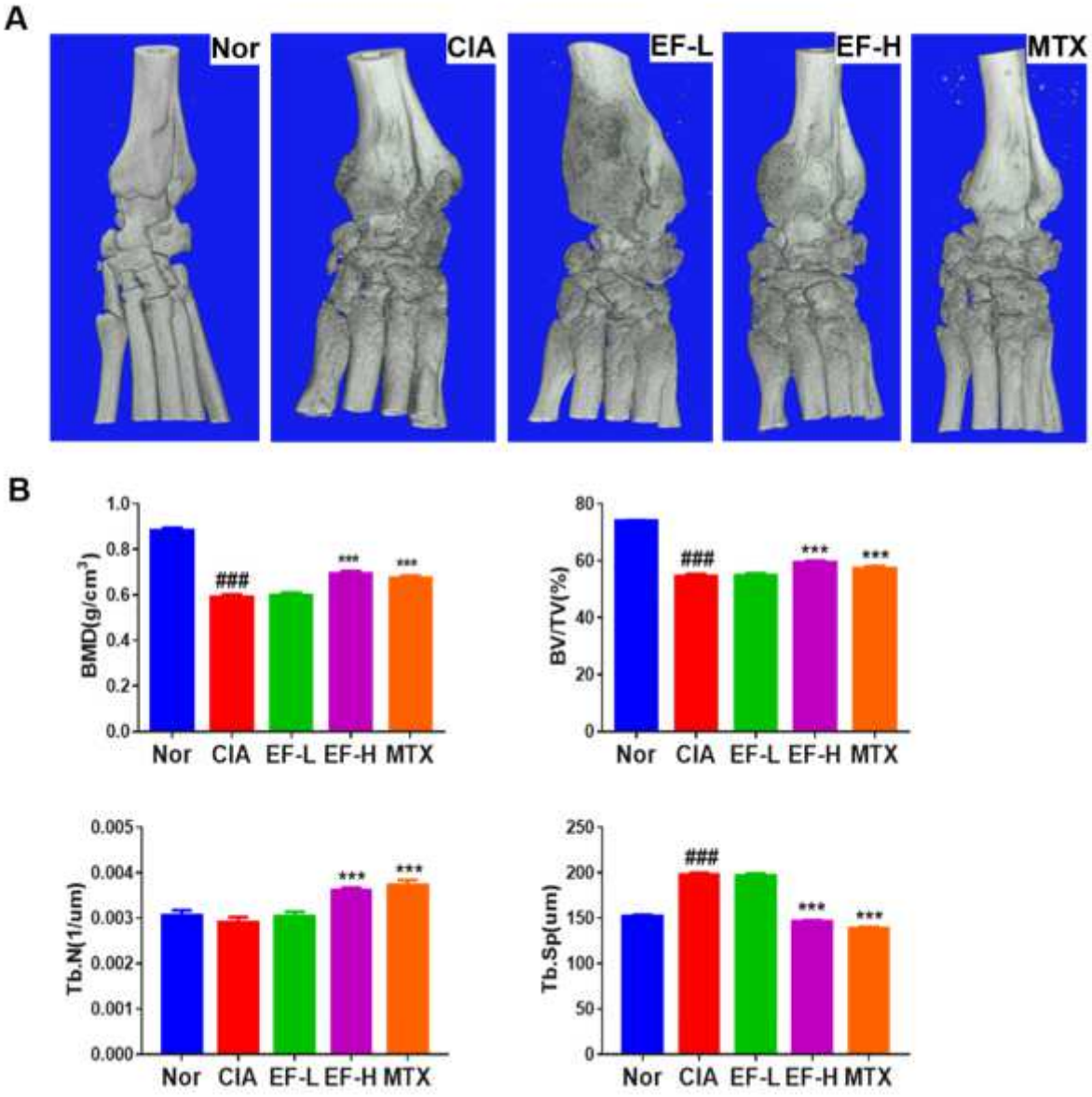

Figure 8

Analysis of micro-computed tomography (micro-CT) data. (A) All drugs were administered orally, and methotrexate (MTX) was used as a positive agent (1 mg/kg; administered once a day). EF was administered at a dose of 2 g·kg-1·day-1 (EF-L) or 4 g·kg-1·day-1(EF-H). (B) Analysis of bone microstructural parameters, including percentage BMD, BV/TV (%), Tb.N (μm), and Tb.Sp (μm)). Data are represented as mean ± SD (n = 3), *p < 0.05, **p < 0.01, ***p < 0.001, vs. CIA animal (CIA rats without EF and MTX treatment), #p < 0.05, ##p < 0.01, ###p < 0.001, vs. normal group.

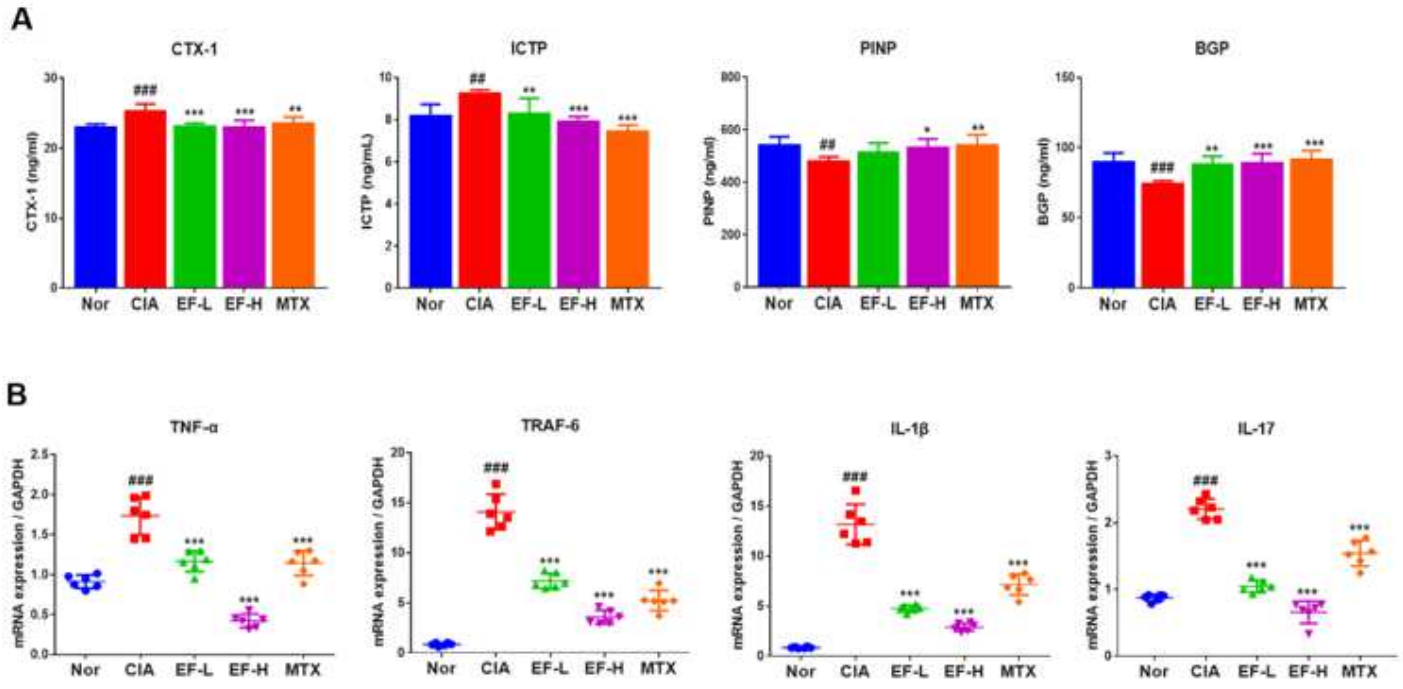

Figure 9

The levels of inflammatory cytokines in the serum and spleen of rats, as detected by ELISA and RT-qPCR. All drugs were administered orally, and methotrexate (MTX) was used as a positive agent (0.3 mg/kg, administered once daily). EF was administered at a dose of 2 g·kg-1·day-1 (EF-L) and 4 g·kg-1·day-1(EF-H). (A) The effects of EF on the serum levels of CTX-1, ICTP, PINP, and BGP, in CIA rats. (B) The effects of EF on the levels of TNF-α, TRAF-6, IL-1β, and IL-17, in the serum of CIA rats. Data are represented as mean ± SD (n = 6), *p < 0.05, **p < 0.01, ***p < 0.001, vs. CIA animal (CIA rats without EF and MTX treatment), #p < 0.05, ##p < 0.01, ###p < 0.001, vs. normal group.

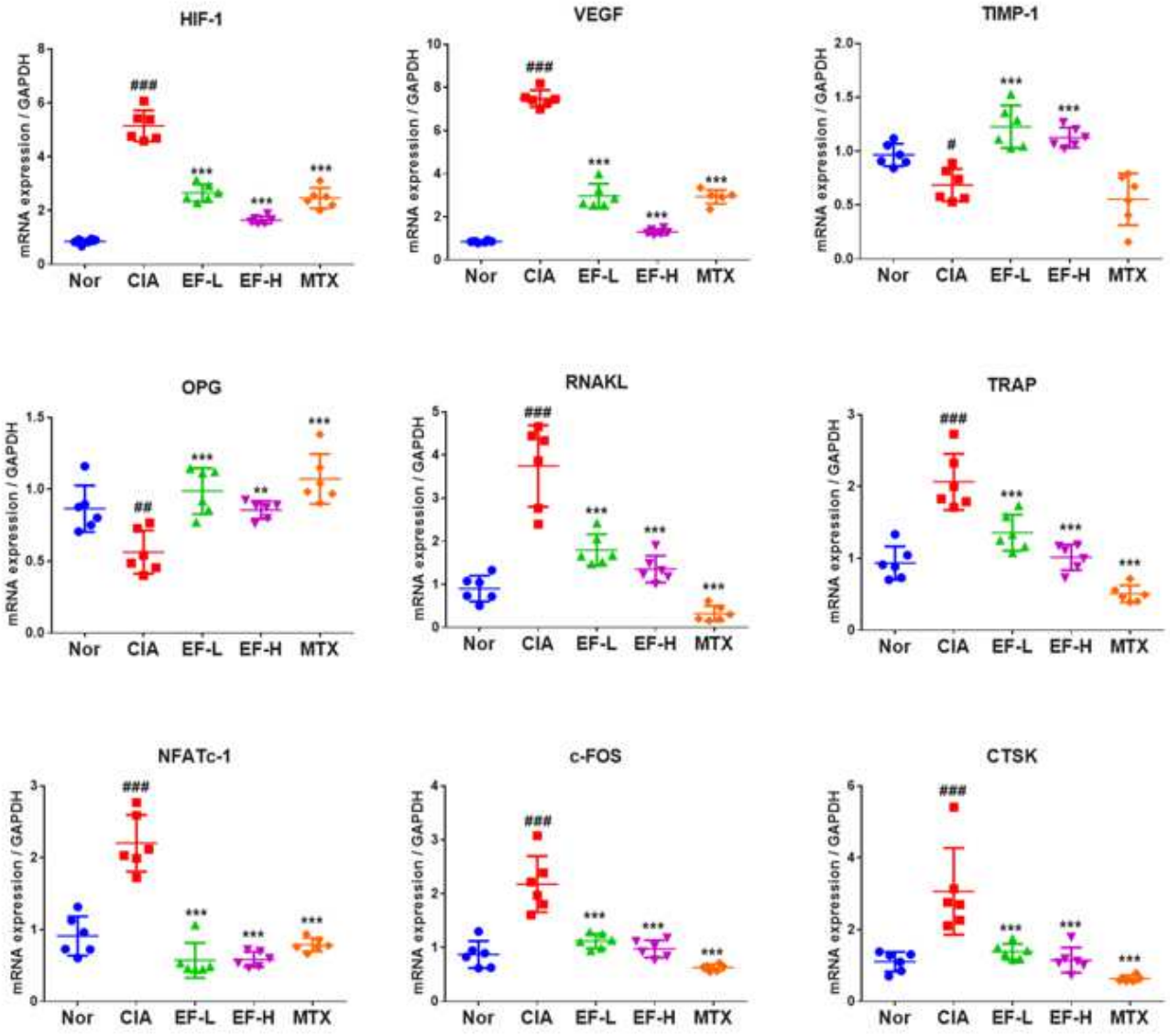

Figure 10

The expression levels of indicators of bone metabolism in rat cartilage tissue, as determined by RT-qPCR. All drugs were administered orally, and methotrexate (MTX) was used as a positive agent (0.3 mg/kg, administered once daily). EF was administered at a dose of 2 g·kg-1·day-1 (EF-L) and 4 g·kg-1·day-1(EF-H). Data are represented as mean ± SD (n = 6), *p < 0.05, **p < 0.01, ***p < 0.001, vs. CIA animal (CIA rats without treatment by EF and MTX), #p < 0.05, ##p < 0.01, ###p < 0.001, vs. normal group.

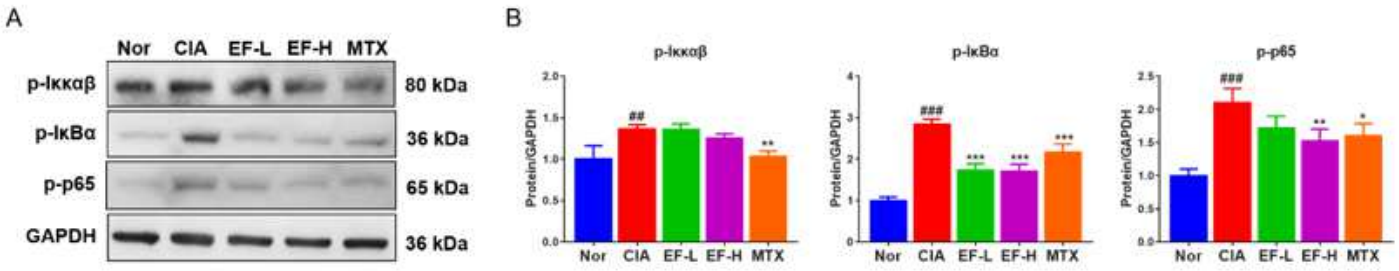

Figure 11

Western blot analysis was conducted to assess the expression levels of p-p65 NF-κB, p-Ικκαβ, and p-IκBα. All drugs were administered orally, and methotrexate (MTX) was used as a positive agent (0.3 mg/kg, administered once daily). EF was administered at a dose of 2 g·kg-1·day-1 (EF-L) and 4 g·kg-1·day-1(EF-H). Data are represented as mean ± SD (n = 3), *p < 0.05, **p < 0.01, ***p < 0.001, vs. CIA animal (CIA rats without treatment by EF and MTX), #p < 0.05, ##p < 0.01, ###p < 0.001, vs. normal group.

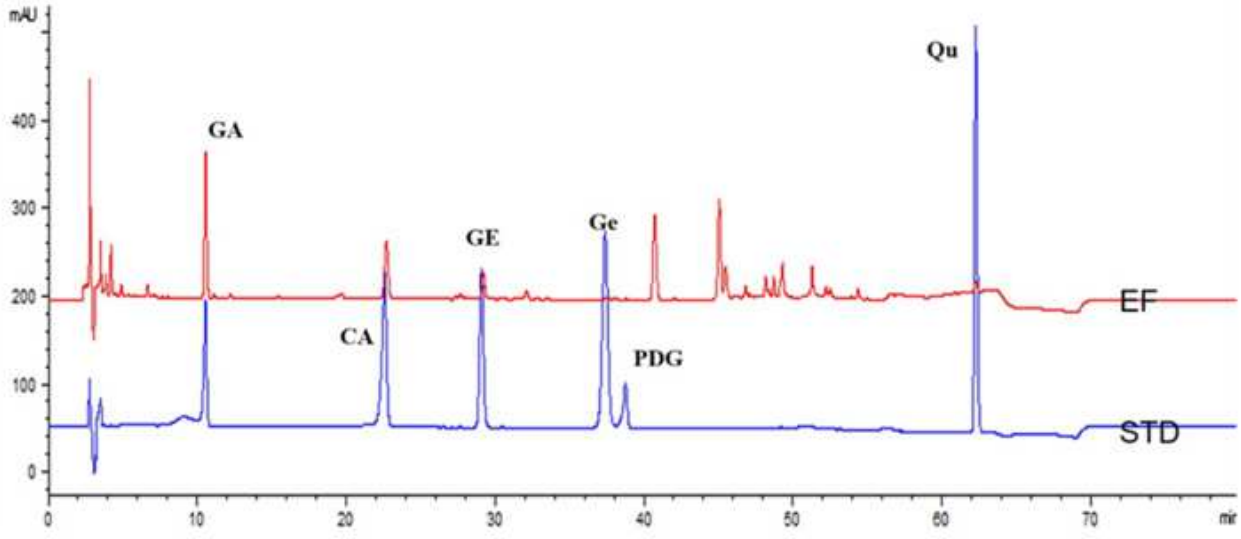

order	ingredient	Content (mg/g)
GA	geniposidic acid	4.3
CA	chlorogenic acid	1.5
Qu	quercetin	0.2

Figure 12

HPLC chromatogram of chemical constituents in the ethanol extract of male flower of Eucommia ulmoides Oliv. The instrument is Angilent 1260. HPLC conditions: Mobile phase acetonitrile (phase A),

0.1% phosphoric acid aqueous solution (phase B), gradient elution. 0 min 4% A; 5 min 10% A; 35 min 23% A; 45 min 60% A; 50 min 90% A; 60 min 90% A; 60.01–80 min 4% A. Cosmosil 5C12 AR-II column, wavelength: 238 nm; 1.0 mL/min; T: 25°C. Sample preparation: The male flower of Eucommia ulmoides Oliv. (EF) was purchased from Shanghai Kangqiao Chinese Medicine Tablet Co., Ltd., (Shanghai, China) and identified as dried male flower of Eucommiaul moides Oliv. by Associate Professor Wu Jin-Rong from the Department of Pharmacognosy, School of Chinese Materia Medica, Shanghai University of Chinese Medicine. EF was extracted twice using 70% ethanol (1:8, w/v for 1 h), filtered and vacuum dried to await experimentation. The concentration of the extract was 1 g/mL. Transfer to a 100-mL volumetric flask, and bring to volume. Reference substance: pinoresinol diglucoside 0.0816 mg/mL + geniposidic acid 0.0368 mg/mL + chlorogenic acid 0.038 mg/mL + geniposide 0.0396 mg/mL + genipin 0.0408 mg/mL + quercetin 0.0204 mg/mL. Note: geniposidic acid for GA; chlorogenic acid for CA; geniposide for GE; genipin for Ge; pinoresinol diglucoside for PDG; quercetin for Qu.

Supplementary Files

This is a list of supplementary files associated with this preprint. Click to download.

- Graphicalabstract.docx